Image Restoration by Group Sparsity with Union of Hierarchical DirLOTs

Kazuki Sakashita* and Shogo Muramatsu†
* Graduate School of Science and Technology, Niigata Univ., Japan
† Faculty of Engineering, Niigata Univ., Japan

***Abstract*—In this study, we propose to introduce group sparse regularization with multiple Directional Lapped Orthogonal Transforms (DirLOTs) for image restoration. Sparse signal restoration has shown its effectiveness in a wide variety of fields. While ℓ_1-norm regularization is typically used in sparse restoration, a group sparse regularization can restore signals more effectively if sparse structure in signals is organized into groups. As a previous research, a group sparse regularization with dependency between discrete wavelet transform (DWT) coefficients has been proposed and the significance is demonstrated. Since DirLOTs are redundant and symmetric, more effective sparse restoration can be expected than ordinary DWTs. In this work, we introduce group sparse regularization into image restoration with multiple DirLOTs, where the symmetric property is utilized. Through simulations, the restoration performance of the proposed method is shown and the significance is confirmed.**

I. Introduction

Developing of sensing technology, acquisition of data in various situation becomes possible. To use sensing data effectively, high quality data reconstruction is needed. However, restoring data which are measured under severe environment is not trivial. In this situation, prior knowledge that signals are sparsely represented has shown the effectiveness in many reconstruction problems [1]. Therefore, incorporating a prior into a restoration model is important to restore high quality signals.

Fig. 1 shows a framework of sparsity-aware restoration problem. Let an observation image $\mathbf{v} \in \mathbb{R}^K$ be represented by

$$\mathbf{v} = \mathbf{P}\mathbf{u}^\star + \mathbf{w}, \mathbf{w} \sim \mathcal{N}(\mathbf{0}, \sigma_w^2 \mathbf{I}), \tag{1}$$

where $\mathbf{u}^\star \in \mathbb{R}^J$ is an unknown clean image, $\mathbf{P} \in \mathbb{R}^{K \times J}$ is a measurement process and $\mathbf{w} \in \mathbb{R}^K$ is additive white Gaussian noise (AWGN) with mean $\mathbf{0}$ and covariance $\sigma_w^2 \mathbf{I}$. Image restoration problem is to estimate an image $\mathbf{u}^\star$ from the observation image $\mathbf{v}$. Since the process $\mathbf{P}$ is not invertible typically, this problem is ill-posed. In this case, sparsity as prior knowledge works well for the restoration. As shown in Fig. 1, the restored image $\hat{\mathbf{u}}$ is represented by a dictionary $\mathbf{D} \in \mathbb{R}^{J \times L}$ and transform coefficients $\hat{\mathbf{s}} \in \mathbb{R}^L$ as $\hat{\mathbf{u}} = \mathbf{D}\hat{\mathbf{s}}$. Based on this assumption, the problem of estimating coefficients $\hat{\mathbf{s}}$ from an observed image $\mathbf{v}$ is set as follows:

$$\hat{\mathbf{s}} = \arg\min_{\mathbf{s}} \frac{1}{2}\|\mathbf{P}\mathbf{D}\mathbf{s} - \mathbf{v}\|_2^2 + \lambda\rho(\mathbf{s}), \tag{2}$$

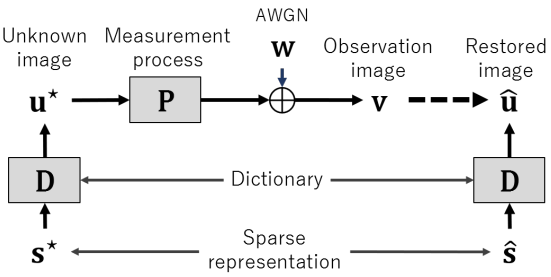

Fig. 1. Framework of sparsity-aware restoration problem.

where $\|\cdot\|_2$ is the ℓ_2-norm, $\rho(\cdot)$ is a regularization term and $\lambda \geq 0$ is a regularization parameter. For sparse representation, the ℓ_1-norm regularization is typically used and its effectiveness has been confirmed [1]. In recent years, image restoration methods using deep convolutional neural network (CNN) were developed [2], [3]. In these methods, CNN is trained from data and then applied to solve the problem. While these methods have been shown to be effective, they require a huge number of design parameters to train the network.

For representing images, a suitable synthesis dictionary $\mathbf{D}$ is demanded to restore clean images. As classical approach, separable transform such as discrete cosine transform (DCT) and DWT have disadvantage in representing diagonal edges and textures. Contourlets proposed by Do et al. satisfy non-separable property [4]. However, it is difficult to satisfy the tight and symmetric property simultaneously. DirLOT, non-separable lapped orthogonal transform with directional property, can satisfy both of the properties [5]. Furthermore, multiple DirLOTs, which consist of several DirLOTs, can improve sparse representation of images with multiple diagonal edges and textures [6], [7]. The redundancy works effectively to promote the sparsity. In [8], [9], image restoration with the ℓ_1-norm regularization and Poisson denoising were proposed and the effectiveness of multiple DirLOTs was confirmed.

While the ℓ_1-norm regularization was successful in image restoration [8], it ignores the relationship between transform coefficients. Since a dictionary with a hierarchical structure has dependency of coefficients among scales, it is expected to improve the performance. As a previous research, Rao et al. [10] proposed group sparse regularization to use dependency among scales in a hierarchical structure. Note that, since

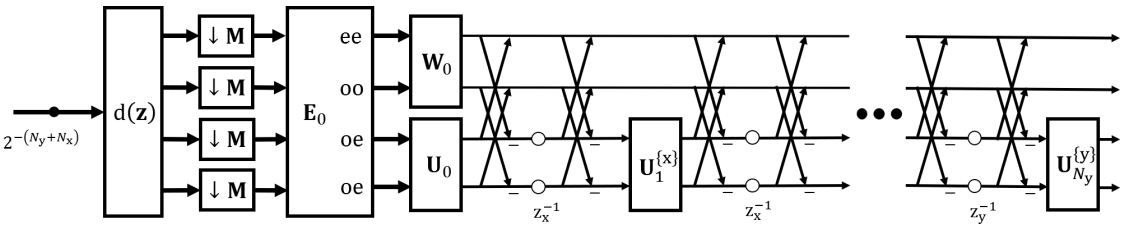

Fig. 2. Lattice structure of a four channel analysis bank of DirLOT, where $\mathbf{d}(\mathbf{z})$ is a 2-D delay chain of size 4×1, $\mathbf{M}$ is the downsampling matrix and is $\mathbf{M} = \mathrm{diag}(M_\mathrm{y}, M_\mathrm{x})$, symbols $\mathbf{W}_0$, $\mathbf{U}_0$ and $\mathbf{U}_{n_d}^{\{d\}}$ are orthonormal matrices of size $M/2 \times M/2$, $\mathbf{E}_0$ is an $M \times M$ matrix directly given by the 2-D DCT, z_x^{-1}, and z_y^{-1} are shift operates of the coefficients in the horizontal and vertical direction, respectively.

the symmetric property of DirLOTs do not need a group delay compensation, it is expected to effectively represent the dependency [12].

In this paper, we introduce a group sparse regularization into an image denoising with multiple DirLOTs, where we can utilize the tight and symmetric property. In addition, the proposed method has fewer parameters than the restoration methods with CNN since there is no training. The proposed method is evaluated through its image denoising application. This paper is organized as follows: Section 2 reviews multiple DirLOTs and problem settings for sparsity-aware restoration. Section 3 describes the proposed method. Section 4 evaluates the performance of the proposed method. Finally, the conclusions follow in Section 5.

II. Review of multiple DirLOTs

In this section, let us review DirLOT and problem setting with multiple DirLOTs for sparse representation.

A DirLOT is a non-separable transforms and can simultaneously satisfy the fixed-critically-subsampled, overlapped, orthonormal, symmetric, real-valued and compact support property. In addition, a DirLOT can hold the trend vanishing moments (TVMs) for any direction. The directional property works well for diagonal texture and edge representation [5].

A. Outline of DirLOT

Fig.2 shows the lattice structure of an analysis bank of DirLOT. The polyphase matrix of order $[N_\mathrm{y}, N_\mathrm{x}]^T$ is represented for even M by

$$\mathbf{E}(\mathbf{z}) = \prod_{n_\mathrm{y}=1}^{N_\mathrm{y}} \{\mathbf{R}_{n_\mathrm{y}}^{\{\mathrm{y}\}} \mathbf{Q}(z_\mathrm{y})\} \cdot \prod_{n_\mathrm{x}=1}^{N_\mathrm{x}} \{\mathbf{R}_{n_\mathrm{x}}^{\{\mathrm{x}\}} \mathbf{Q}(z_\mathrm{x})\} \cdot \mathbf{R}_0 \mathbf{E}_0, \quad (3)$$

where $\mathbf{z} = (z_\mathrm{y}, z_\mathrm{x})^T \in \mathbb{C}^2$ is a variable vector in the 2-D Z-transform domain. Matrix $\mathbf{Q}(z_d), \mathbf{R}_0$ and $\mathbf{R}_n^{\{d\}}$ is represented by

$$\mathbf{Q}(z_d) = \frac{1}{2} \begin{pmatrix} \mathbf{I}_{\frac{M}{2}} & \mathbf{I}_{\frac{M}{2}} \\ \mathbf{I}_{\frac{M}{2}} & -\mathbf{I}_{\frac{M}{2}} \end{pmatrix} \begin{pmatrix} \mathbf{I}_{\frac{M}{2}} & \mathbf{0}_{\frac{M}{2}} \\ \mathbf{0}_{\frac{M}{2}} & z_d^{-1} \mathbf{I}_{\frac{M}{2}} \end{pmatrix} \begin{pmatrix} \mathbf{I}_{\frac{M}{2}} & \mathbf{I}_{\frac{M}{2}} \\ \mathbf{I}_{\frac{M}{2}} & -\mathbf{I}_{\frac{M}{2}} \end{pmatrix},$$

$$\mathbf{R}_0 = \begin{pmatrix} \mathbf{W}_0 & \mathbf{0}_{\frac{M}{2}} \\ \mathbf{0}_{\frac{M}{2}} & \mathbf{U}_0 \end{pmatrix}$$

and

$$\mathbf{R}_n^{\{d\}} = \begin{pmatrix} \mathbf{I}_{\frac{M}{2}} & \mathbf{0}_{\frac{M}{2}} \\ \mathbf{0}_{\frac{M}{2}} & \mathbf{U}_n^{\{d\}} \end{pmatrix},$$

where $d \in \{\mathrm{x}, \mathrm{y}\}$ denote a direction. x and y mean horizontal and vertical direction, respectively. In the above expression, the product of sequential matrices is defined by

$$\prod_{n=1}^{N} \mathbf{A}_n = \mathbf{A}_N \mathbf{A}_{N-1} \cdots \mathbf{A}_2 \mathbf{A}_1.$$

$\mathbf{E}_0$ is an $M \times M$ symmetric orthonormal transform matrix given directly through the 2-D separable DCT, where M is the number of channels, i.e. $M = |\det(\mathbf{M})|$. Symbols $\mathbf{W}_0$, $\mathbf{U}_0$ and $\mathbf{U}_{n_d}^{\{d\}}$ denote orthonormal matrices of size $M/2 \times M/2$, which are freely controlled during the design process.

A single DirLOT is not suitable for an image with texture and edges in multiple directions. Thus, multiple DirLOTs, a dictionary consists of several DirLOTs with a different directions, was developed [7]. The dictionary is represented by

$$\mathbf{D} = [\mathbf{\Phi}_{0 \cup \frac{\pi}{2}}^T \quad \mathbf{\Phi}_{\phi_1}^T \quad \mathbf{\Phi}_{\phi_2}^T \quad \cdots \quad \mathbf{\Phi}_{\phi_{C-1}}^T], \quad (4)$$

where $\mathbf{\Phi}_{0 \cup \frac{\pi}{2}}^T$ is an isotropic symmetric orthonormal DWT (ISOWT) with the classical two-order vanishing moments [11] and $\mathbf{\Phi}_{\phi_c}$ for $c \in \{1, 2, \cdots, C-1\}$ is a directional symmetric orthonormal wavelet transforms (DirSOWTs) constructed by DirLOTs with the two-order TVMs for the direction ϕ_c. C denotes the number of DWTs, i.e. the redundancy of dictionary $\mathbf{D}$. $\mathbf{D}$ gives a tight frame with normalized atoms and satisfies $\mathbf{D}\mathbf{D}^T = C\mathbf{I}$. Note that the symmetric property is suitable for grouping the coefficients between scales. In transforms without the symmetric property, the group delays may differ from other scales. Some group delay compensation is needed to adjust the phase shift. While transforms with the symmetric property do not need this kind of group delay compensation. In this sense, DirLOT is suitable for grouping coefficients between scales [12].

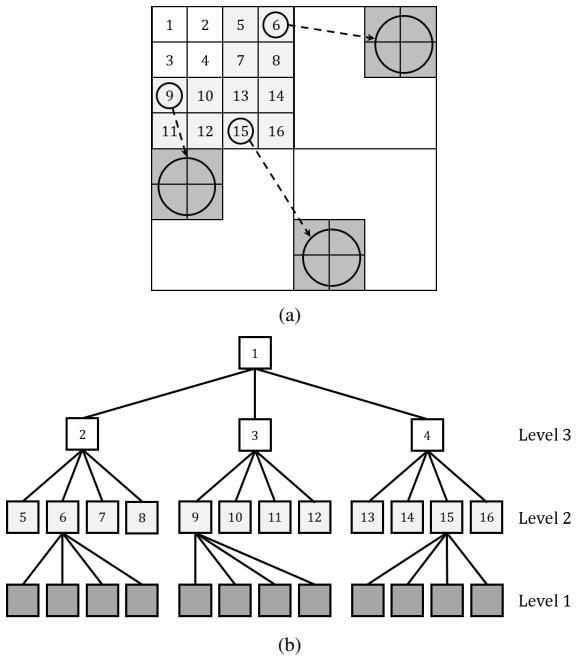

Fig. 3. Illustration of wavelet coefficient dependency. (a) 8×8 montage image using 3-level DWT coefficient. (b) is a dependency model in the case of (a).

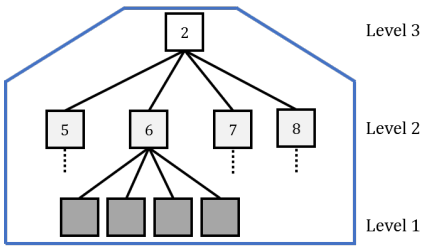

Fig. 4. Illustration of a grouping method to introduce group sparse. This method group the top level parent and the children corresponding to that parent across levels.

Algorithm 1 Proximal gradient method

Input: $\mathbf{v}, \alpha, \lambda, n$
Output: $\hat{\mathbf{u}}$
Initialization :
$n \leftarrow 0$
$\mathbf{x}^{(0)} \leftarrow C^{-1}\mathbf{D}^T\mathbf{P}^T\mathbf{v}$
while $\|\mathbf{s}^{(n)} - \mathbf{s}^{(n-1)}\|_2^2 / \|\mathbf{s}^{(n)}\|_2^2 > \epsilon$ **do**
$\mathbf{s}^{(n+1)} = \mathrm{prox}_{\frac{\lambda}{\alpha}\rho(\cdot)}(\mathbf{s}^{(n)} - \frac{2}{\alpha}(\mathbf{D}^T\mathbf{P}^T(\mathbf{P}\mathbf{D}\mathbf{s}^{(n)} - \mathbf{v})))$
$n = n + 1$
end while
$\hat{\mathbf{u}} \leftarrow \mathbf{D}\mathbf{s}^{(n)}$

B. Problem setting

In sparse representation approach, when the regularization term $\rho(\cdot)$ in (2) is set to ℓ_1-norm, the problem becomes LASSO as follows:

$$\hat{\mathbf{s}} = \arg\min_{\mathbf{s}} \frac{1}{2}\|\mathbf{P}\mathbf{D}\mathbf{s} - \mathbf{v}\|_2^2 + \lambda\|\mathbf{s}\|_1. \tag{5}$$

We proposed to take another regularizer. Coefficients $\mathbf{s}$ can be organized into groups. The following problem setting adopts the mixed $\ell_{1,2}$-norm regularization [13]:

$$\hat{\mathbf{s}} = \arg\min_{\mathbf{s}} \frac{1}{2}\|\mathbf{P}\mathbf{D}\mathbf{s} - \mathbf{v}\|_2^2 + \lambda \sum_{\mathfrak{g}\in\mathfrak{G}} \|\mathbf{s}_{\mathfrak{g}}\|_2, \tag{6}$$

where $\sum_{\mathfrak{g}\in\mathfrak{G}} \|\cdot\|_2$ is the mixed $\ell_{1,2}$-norm, $\mathbf{s}_{\mathfrak{g}}$ denotes a sub vector of $\mathbf{s}$ belonging to the $\mathfrak{g}$-th group and $\mathfrak{G}$ is an index set of the groups.

In sparse representation, while the ℓ_1-norm regularization was effective, it ignores the relationship between transform coefficients. Group sparsity can incorporates this relationship. To use the group sparsity, we need to model a grouping structure.

III. Introduction of Group Sparsity

In this section, let us describe our proposed group sparse regularization for an union of multiple hierarchical DirLOTs.

When a dictionary $\mathbf{D}$ has a hierarchical structure, coefficients may have some dependency, which shows the tendency that large coefficients prone to appear across scales. The dependency was modeled as [15]. Fig. 3 shows an example of a model with a DWT dictionary. As shown in Fig. 3, the model connects the coefficients of parents and children. Based on this model, grouping methods for group sparse regularization are considered in [10].

Fig. 4 shows the grouping method in this work. As shown in Fig. 4, a parent at the top level and all children corresponding to the parent across scale are grouped. By applying this grouping to all the coefficients, group sparse regularization is realized.

Since this grouping yields non-overlapping groups, the proximal map of the mixed $\ell_{1,2}$-norm is represented by

$$[\mathrm{prox}_{\frac{\lambda}{\alpha}\|\cdot\|_{1,2}}(\mathbf{s})]_{\mathfrak{g}} = \frac{\mathbf{s}_{\mathfrak{g}}}{\|\mathbf{s}_{\mathfrak{g}}\|_2}\max\left(\|\mathbf{s}_{\mathfrak{g}}\|_2 - \frac{\lambda}{\alpha}, 0\right). \tag{7}$$

Thus, the problem in (6) can be solved by the proximal gradient method [14] shown in Algorithm 1. In Algorithm 1, α is the Lipschitz constant of ∇f. Since our dictionary $\mathbf{D}$ yields a tight frame and $\mathbf{D}\mathbf{D}^T = C\mathbf{I}$, the Lipschitz constant is given by

$$\alpha = 2C\lambda_{\max}(\mathbf{P}^T\mathbf{P}), \tag{8}$$

where $\lambda_{\max}(\cdot)$ denotes the maximum eigenvalue.

IV. Performance Evaluation

In this section, we evaluate the proposed method through some experiments on image denoising. To verify the performance, the image restoration performance with the ℓ_1-norm regularization and BM3D [16] are also shown for reference. We used the proximal gradient method for the experiments. The stop condition of the algorithm is set to a fixed iteration

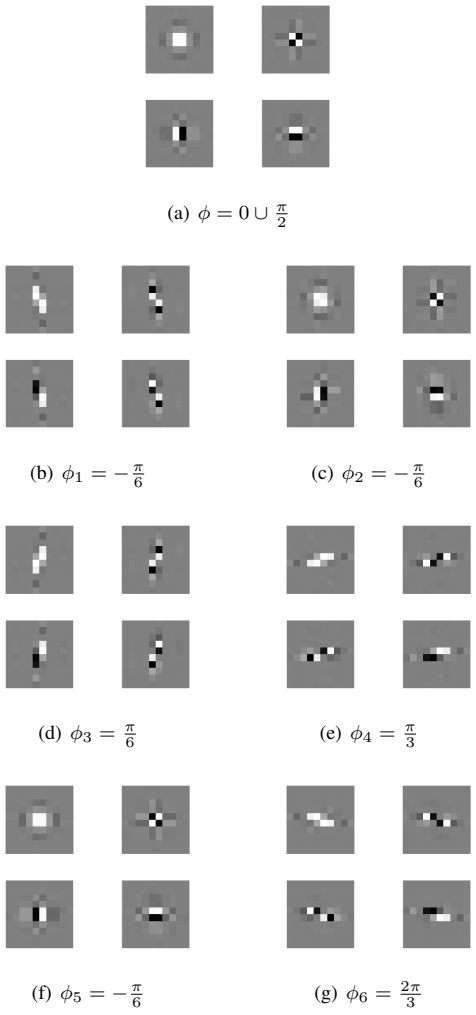

(a) $\phi = 0 \cup \frac{\pi}{2}$

(b) $\phi_1 = -\frac{\pi}{6}$ (c) $\phi_2 = -\frac{\pi}{6}$

(d) $\phi_3 = \frac{\pi}{6}$ (e) $\phi_4 = \frac{\pi}{3}$

(f) $\phi_5 = -\frac{\pi}{6}$ (g) $\phi_6 = \frac{2\pi}{3}$

Fig. 5. Bases of DirLOTs used in this experiment. (a) ISOWT, (b) - (g) The bases of DirLOTs designed for angles in (9). The polyphase order and decimation matrix is set to $[N_y, N_x]^T = [4, 4]^T$ and $\mathbf{M} = \mathrm{diag}(M_y, M_x) = (2, 2)$, respectively.

number of 20 times. The regularization parameter is set by hand. The multiple DirLOTs consists of one ISOWT and four DirSOWTs of polyphase order $[N_{\mathrm{y}}, N_{\mathrm{x}}]^T = [4, 4]^T$ and decimation matrix $\mathbf{M} = \mathrm{diag}(M_{\mathrm{y}}, M_{\mathrm{x}}) = (2, 2)$. We select the following six angles for ϕ_c in (4) as

$$\phi_c \in \left\{-\frac{\pi}{6}, 0, \frac{\pi}{6}, \frac{\pi}{3}, \frac{\pi}{2}, \frac{2\pi}{3}\right\}, \tag{9}$$

Fig. 5 shows the bases of DirLOTs designed for angles in (9). The number of tree levels of the multiple DirLOTs is set to 4. To generate an observation image, we use the 2-D Gaussian filter with standard deviation $\sigma_b = 2.0$ and AWGN with standard deviation $\sigma_w \in \{20, 30, 40\}$. The restoration performance is evaluated by the peak-signal to noise ratio (PSNR) and structural similarity index measure (SSIM). The PSNR is given by

TABLE I
COMPARISON OF PSNR AMONG THREE METHODS FOR VARIOUS PICTURES AND AWGN WITH STANDARD DEVIATION σ_{w}. THE VALUE IN THE PARENTHESIS INDICATE THE REGULARIZATION PARAMETER λ. THE NUMBER OF TREE LEVELS OF THE MULTIPLE DIRLOTS IS SET TO 4.

Image	σ_w	PSNR		
		ℓ_1-norm	BM3D	Proposal
Lena	20	27.57 (0.054)	**27.92**	27.77 (0.20)
	30	26.60 (0.12)	**27.07**	26.79 (0.33)
	40	25.72 (0.19)	**26.26**	25.95 (0.44)
Baboon	20	20.80 (0.028)	20.62	**20.88 (0.13)**
	30	20.41 (0.079)	20.28	**20.53 (0.25)**
	40	20.15 (0.15)	20.07	**20.28 (0.38)**
Barbara	20	23.13 (0.051)	**23.32**	23.16 (0.19)
	30	22.72 (0.12)	**22.96**	22.76 (0.32)
	40	22.41 (0.19)	**22.66**	22.44 (0.45)
Goldhill	20	26.40 (0.055)	25.96	**26.64 (0.19)**
	30	25.67 (0.12)	25.70	**25.92 (0.32)**
	40	25.04 (0.20)	**25.24**	25.23 (0.44)
Man	20	25.90 (0.046)	26.01	**26.03 (0.18)**
	30	25.06 (0.11)	25.20	**25.25 (0.30)**
	40	24.48 (0.18)	24.61	**24.63 (0.43)**
Boat	20	25.01 (0.039)	25.15	**25.24 (0.16)**
	30	24.23 (0.096)	24.29	**24.52 (0.28)**
	40	23.62 (0.17)	23.68	**23.89 (0.41)**

TABLE II
COMPARISON OF SSIM AMONG THREE METHODS FOR VARIOUS PICTURES AND AWGN WITH STANDARD DEVIATION σ_{w}. THE VALUE IN THE PARENTHESIS INDICATE THE REGULARIZATION PARAMETER λ. THE NUMBER OF TREE LEVELS OF THE MULTIPLE DIRLOTS IS SET TO 4.

Image	σ_w	SSIM		
		ℓ_1-norm	BM3D	Proposal
Lena	20	0.744 (0.054)	**0.779**	0.755 (0.20)
	30	0.720 (0.12)	**0.761**	0.728 (0.33)
	40	0.694 (0.19)	**0.746**	0.701 (0.44)
Baboon	20	0.423 (0.028)	0.379	**0.424 (0.13)**
	30	0.387 (0.079)	0.347	**0.391 (0.25)**
	40	0.366 (0.15)	0.332	**0.371 (0.38)**
Barbara	20	0.604 (0.051)	**0.631**	0.605 (0.19)
	30	0.582 (0.12)	**0.612**	0.581 (0.32)
	40	0.565 (0.19)	**0.598**	0.564 (0.45)
Goldhill	20	0.632 (0.055)	0.630	**0.642 (0.19)**
	30	0.604 (0.12)	0.605	**0.615 (0.32)**
	40	0.586 (0.20)	0.588	**0.593 (0.44)**
Man	20	0.655 (0.046)	**0.671**	0.661 (0.18)
	30	0.625 (0.11)	**0.642**	0.632 (0.30)
	40	0.604 (0.18)	**0.623**	0.608 (0.43)
Boat	20	0.627 (0.039)	**0.644**	0.642 (0.16)
	30	0.597 (0.096)	**0.6122**	0.6121 (0.28)
	40	0.578 (0.17)	**0.593**	0.590 (0.41)

$$\begin{aligned} \mathrm{PSNR} &= 10 \log_{10} \frac{255^2}{\mathrm{MSE}} \\ \mathrm{MSE} &= \frac{1}{J} \sum_{\mathrm{j}=1}^{J} (u_j - u_j^\star)^2, \end{aligned}$$

where u_j and $u_j^\star$ are the j-th element of $\mathbf{u}$ and $\mathbf{u}^\star$. The SSIM is computed as follows:

$$\begin{aligned} \mathrm{SSIM} &= \frac{(2\mu_{\mathbf{u}}\mu_{\mathbf{u}^\star} + c_1)(2\sigma_{\mathbf{u}\mathbf{u}^\star} + c_2)}{(\mu_{\mathbf{u}}^2 + \mu_{\mathbf{u}^\star}^2 + c_1)(\sigma_{\mathbf{u}} + \sigma_{\mathbf{u}^\star} + c_2)} \\ c_1 &= 1.0 \times 10^{-4},\ c_2 = 3.0 \times 10^{-4}, \end{aligned}$$

(a) Original (b) Observation (18.59 dB) (c) BM3D (20.62 dB) (d) ℓ_1-norm (20.80 dB) (e) Proposal (20.88 dB)

Fig. 6. Image denoising result when $\sigma_w = 20$ for "Baboon". (a) Original image, (b) Observation image (PSNR: 18.59 dB), (c) Restored image with BM3D (PSNR: 20.62 dB), (d) Restored image with the ℓ_1-norm regularization (PSNR: 20.80 dB), (d) Restored image with the proposed method (PSNR: 20.88 dB).

(a) Original (b) Observation (21.05 dB) (c) BM3D (25.70 dB) (d) ℓ_1-norm (25.67 dB) (e) Proposal (25.92 dB)

Fig. 7. Image denoising result when $\sigma_w = 20$ for "Goldhill". (a) Original image, (b) Observation image (PSNR: 21.05 dB), (c) Restored image with BM3D (PSNR: 25.70 dB), (d) Restored image with the ℓ_1-norm regularization (PSNR: 25.67 dB), (d) Restored image with the proposed method (PSNR: 25.92 dB).

(a) Original (b) Observation (20.80 dB) (c) BM3D (26.01 dB) (d) ℓ_1-norm (25.90 dB) (e) Proposal (26.03 dB)

Fig. 8. Image denoising result when $\sigma_w = 20$ for "Man". (a) Original image, (b) Observation image (PSNR: 20.80 dB), (c) Restored image with BM3D (PSNR: 26.01 dB), (d) Restored image with the ℓ_1-norm regularization (PSNR: 25.90 dB), (d) Restored image with the proposed method (PSNR: 26.03 dB).

where $\mu_{\mathbf{u}}, \mu_{\mathbf{u}^\star}$ are the average of $\mathbf{u}, \mathbf{u}^\star$, $\sigma_{\mathbf{u}}, \sigma_{\mathbf{u}^\star}$ are the variance of $\mathbf{u}, \mathbf{u}^\star$ and $\sigma_{\mathbf{u}\mathbf{u}^\star}$ is the co-variance of $\mathbf{u}$ and $\mathbf{u}^\star$.

A. Experimental results

Tables I, II shows PSNRs and SSIMs from the experiments respectively. Figs. 6-8 also shows the restored images degraded by AWGN with standard deviation $\sigma = 20$. In Table I, the proposed method archives better PSNR than the ℓ_1-norm approach. It is confirmed that the group sparse regularization improves the image restoration performance. In Figs. 6-8, compared to BM3D, the proposed method shows comparable performance and is superior especially for images with detailed edges and textures to the others.

V. Conclusions

In this paper, we introduced group sparse regularization into an image restoration with multiple DirLOTs. Through simulations, it was confirmed that the proposed method improve the restoration performance. In the future, we will apply subband adaptive method such as [17] to the proposed method.

Acknowledgment

This work was supported by JSPS KAKENHI Grant Number JP19H04135.

References

[1] Z. Zhang, Y. Xu, J. Yang, X. Li and D. Zhang, "A survey of sparse representation: algorithms and applications," IEEE access, vol.3, pp.490-530, 2015.

[2] K. Zhang, W. Zuo, Y. Chen, D. Meng, and L. Zhang, "Beyond a Gaussian Denoiser Residual Learning of Deep CNN for Image Denoising," IEEE Trans. Image Process., vol.26, pp.3142–3155, 2017.

[3] D. Ulyanov, A. Vedaldi, V. Lempitsky, "Deep Image Prior," Proc. of IEEE Computer Vision and Pattern Recognition, pp.9446–9454, June 2018.

[4] A.L. da Cunha, J. Zhou, and M.N. Do, "The nonsubsampled contourlet transform: Theory, design, and applications," IEEE Trans. Image Process., vol.15, no.10, pp.3089–3101, Oct. 2006

[5] S. Muramatsu, D. Han, T. Kobayashi and H. Kikuchi, "Directional lapped orthonormal transform: Theory and design," IEEE Trans. Image Process., vol.21, no.5, pp.2434-2448, May 2012.

[6] S. Muramatsu, D. Han, "Image denoising with union of directional orthonormal DWTs," Proc. of IEEE International Conference on Acoustics, Audio and Signal Processing, pp.1089–1092, March 2012.
[7] S. Muramatsu, "SURE-LET image denoising with multiple directional LOTs," Proc. of Picture Coding Symposium, May 2012.
[8] N. Aizawa, S. Muramatsu and Masahiro Yukawa, "Image restoration with multiple DirLOTs," IEICE Trans. on Fundamentals, vol.E96-A, no.10, pp.1954-1961, Oct. 2013.
[9] C. Zhiyu, S. Muramatsu, "SURE-LET poisson denoising with multiple directional LOTs," IEICE Trans. on Fundamentals, vol.E98-A, no.8, pp. 1820-1828, Aug. 2015.
[10] N. Rao, R. Nowak, S. Wright, and N. Kingsbury, "Convex approaches to model wavelet sparsity patterns," Proc. of IEEE International Conference on Image Processing, Sept. 2011.
[11] T. Kobayashi, S. Muramatsu and H. Kikuchi, "Two-degree vanishing moments on 2-D non-separable GenLOT," Proc. of Int. Symp. on Intelligent Signal Proc. and Communication Systems, pp.248–251, Dec. 2009.
[12] L. Florian, T. Blu and M. Unser. "A new SURE approach to image denoising: Interscale orthonormal wavelet thresholding," IEEE Transactions on image processing, vol.16, pp.593-606, 2007.
[13] M. Yuan, Y. Lin, "Model selection and estimation in regression with grouped variables," Journal of the Royal Statistical Society: Series B (Statistical Methodology), vol.68, no.1, pp.49-67, 2006.
[14] I. Daubechies, M. Defrise, and C. Mol, "An iterative thresholding algorithm for linear inverse problems with a sparsity constraint," Communications on Pure and Applied Mathematics, vol.57, pp.1413–1457, 2004.
[15] M. Crouse, R. Nowak and R. Baraniuk, "Wavelet-Based Statistical Signal Processing Using Hidden Markov Models," IEEE Transactions on Signal Processing, vol.46, no.4, 1998.
[16] A. Danielyan, V. Katkovnik and K. Egiazarian, "BM3D frames and variational image deblurring," IEEE Transactions on Image Processing, vol.21, pp.1715-1728, 2012.
[17] Y. Zhang, N. Kingsbury, "Improved Bounds for Subband-adaptive Iterative Shrinkage/Thresholding Algorithms", IEEE Trans on Image Processing, vol.22, no.4, pp.1373-1381, April 2013.